J. Anat. (2000) **197**, pp. 61–76, with 9 figures Printed in the United Kingdom

Review

Using diagnostic radiology in human evolutionary studies

FRED SPOOR[1], NATHAN JEFFERY[1] AND FRANS ZONNEVELD[2]

[1] *Evolutionary Anatomy Unit, Department of Anatomy and Developmental Biology, University College London, UK, and*
[2] *Department of Radiology, Utrecht University Hospital, The Netherlands*

(*Accepted 20 December 1999*)

ABSTRACT

This paper reviews the application of medical imaging and associated computer graphics techniques to the study of human evolutionary history, with an emphasis on basic concepts and on the advantages and limitations of each method. Following a short discussion of plain film radiography and pluridirectional tomography, the principles of computed tomography (CT) and magnetic resonance imaging (MRI) and their role in the investigation of extant and fossil morphology are considered in more detail. The second half of the paper deals with techniques of 3-dimensional visualisation based on CT and MRI and with quantitative analysis of digital images.

Key words: Human evolution; computed tomography; magnetic resonance imaging; 3-D visualisation; hominin fossils; fetal morphology.

INTRODUCTION

Within a year of the discovery of x-rays in November 1895 radiography was applied to the study of both vertebrate and invertebrate fossils (Brühl, 1896). For the first time, it was possible for paleontologists to assess the internal morphology of rare and valuable specimens in a nondestructive way. Paleoanthropology almost immediately embraced radiography as an analytical tool, and radiographs appear in many of the early monographs describing hominin fossils, such as the Krapina Neanderthals (Gorjanovic-Kramberger, 1906) and the Mauer mandible (Schoetensack, 1908).

More recently the development of computed tomography (CT), in combination with increasingly sophisticated computer graphics applications, has provided a range of new opportunities for the qualitative and quantitative study of fossil morphology that were not available to researchers using conventional radiography. Magnetic resonance imaging (MRI), the 20th century's second major innovation in diagnostic imaging, provides excellent visualisation of soft-tissue structures, but is not suitable for imaging either extant or fossil skeletal morphology. MRI can nevertheless be of great value to human evolutionary studies when used in comparative and functional analyses that relate soft tissues, such as the brain or the muscular system, to bony morphology. Moreover, it can be used to investigate the ontogeny of the skeletal system as a means of understanding the developmental basis of phylogenetic change.

This paper gives an overview of imaging techniques that are particularly relevant to the study of human evolution, and provides an introduction for researchers who do not have a background in either radiology or medical physics. It thus follows in the footsteps of earlier reviews with a similar scope, such as Jungers & Minns (1979), Tate & Cann (1982), Ruff & Leo (1986) and Vannier & Conroy (1989). The focus is on CT and MRI, because both modalities are technically more complex and less straightforward in practical use than conventional radiography. The emphasis is on the basic concepts and on the advantages and limitations of their use, rather than on the underlying technology or on the presentation of the results of previous imaging-based research. Expanding on this paper, Spoor et al. (2000) give a more

Correspondence to Dr Fred Spoor, Department of Anatomy & Developmental Biology, University College London, Rockefeller Building, University Street, London WC1E 6JJ, UK.

technical description of CT and MRI and provide a practical guide for those who wish to apply these imaging techniques in morphological research.

PLAIN FILM RADIOGRAPHY

In conventional, or plain-film, radiography an object is placed between an x-ray source and x-ray sensitive film. The image of the object thus formed represents the distribution and degree of integral attenuation of the x-rays in their passage through the object. Thus, all structures in the path of the x-ray beam are superimposed in the image and cannot be distinguished (Fig. 1*a*). Conventional radiographs therefore provide only limited information about complex 3-dimensional (3-D) objects. Moreover, in the case of fossils morphological information is blocked out by the presence of sedimentary matrix of a higher density (x-ray opacity or attenuation) than that of the fossil itself (see examples in Wind & Zonneveld, 1985). X-rays emerge as a diverging conical beam from the source and the radiographic projection will therefore tend to show a variable degree of distortion. This can be minimised by maximising the source-to-object distance relative to the object-to-film distance, and by using collimators which transmit only parallel x-rays. Compared with medical CT and MRI, conventional radiography has the advantages of higher spatial resolution (ability to resolve small details), and ease of use and cost. In addition to the effects of distortion and the superimposition of structures its major disadvantage is its relatively low contrast resolution (ability to resolve small density differences).

Given the limitations, conventional radiography is most useful when applied to aspects of morphology with relatively simple shapes, such as the dentition (e.g. Skinner & Sperber, 1982; Dean et al. 1986; Wood et al. 1988) and postcranial bones (e.g. Ruff, 1989; Trinkaus & Ruff, 1989; Runestad et al. 1993; Macchiarelli et al. 1999). Moreover, lateral radiographs have traditionally played a central role in studies of the comparative anatomy of primate cranial form (e.g. Angst, 1967; Swindler et al. 1973; Dmoch, 1975, 1976; Cramer, 1977; Ravosa, 1988; Ross & Ravosa, 1993; Lieberman, 1998; Lieberman & McCarthy, 1999; Spoor et al. 1999). They illustrate phylogenetically important aspects of cranial form, such as basicranial flexion and the relationship between the neurocranium and the facial complex. An advantage, inherent to the superimposition effect in radiographs, is that a wide range of structures, for example the palate, the orbits and aspects of the midline cranial base, can be compared using a single image. A drawback, on the other hand, is that the focus on cranial morphology as projected onto a single sagittal plane tends to portray evolutionary change as a 2-D rather than a 3-D process. Some studies, however, have used radiographs with an axial projection to consider morphological change in the transverse plane (Putz, 1974; Dean & Wood, 1981).

Pluridirectional tomography is a special form of radiography that was invented in the 1930s in an attempt to solve the problems associated with the superimposition of morphology. In this technique both the x-ray source and the film are moved in opposite directions during exposure, which results in blurring of all details except in one focal plane. Only a few studies have used this technique to investigate fossils (e.g. Fenart & Empereur-Buisson, 1970; Price

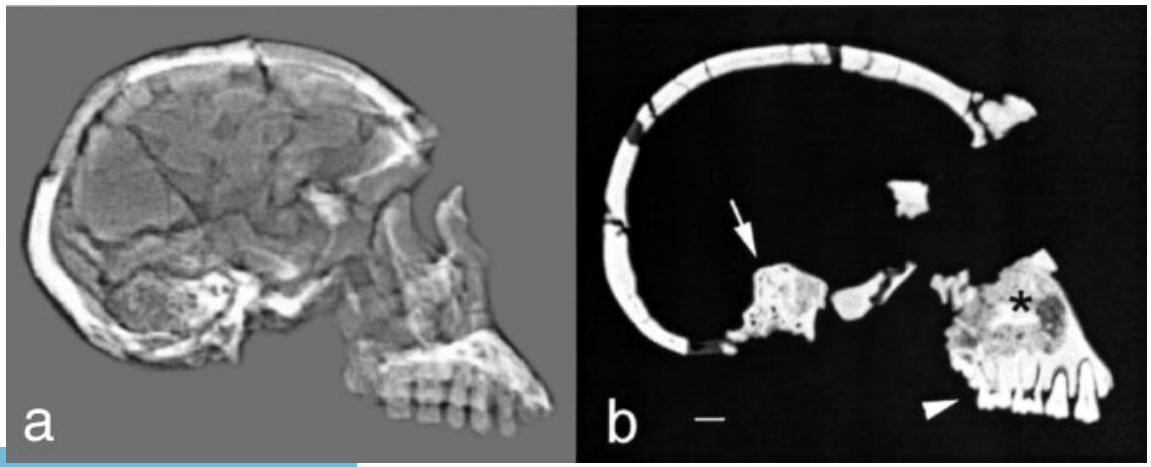

Fig. 1. Imaging the immature *Homo ergaster* cranium KNM-WT15000 (after Spoor et al. 2000). (*a*) Lateral radiograph, (*b*) parasagittal CT scan at the level of the right dental row and inner ear (slice thickness 1 mm). Unlike the radiograph, the CT scan has the ability to distinguish between fossil bone and the sedimentary matrix in the maxillary sinus (∗), and to resolve details such as the root canals of the molars (arrowhead), and structures of the bony labyrinth (arrow). Bar, 10 mm.

& Molleson, 1974; Hotton et al. 1976; Wind & Zonneveld, 1985). Tomography is also the key technique of the so-called vestibular method, in which cranial morphology in lateral projection is compared using a reference plane defined by the lateral semicircular canals of the inner ear (see Fenart & Pellerin, 1988, for a review of this method and its applications).

COMPUTED TOMOGRAPHY (CT)

Since its development (Hounsfield, 1973), CT has taken over from conventional radiography and pluridirectional tomography as the imaging method of choice when investigating complex skeletal morphology. In medical CT scanners an x-ray source and an array of detectors rotate about the specimen and measure its attenuation within the confines of a slice-shaped volume in a great number of directions using a fan beam (Fig. 2). By repositioning the specimen the plane in which measurements are taken can be changed. Digital cross-sectional images, which map the different degrees of attenuation in the slice (expressed as 'CT numbers'), are calculated from the measurements and are shown on a computer monitor using a grey scale with black representing the lowest density and white the highest density (see Newton & Potts, 1981; Swindell & Webb, 1992, for reviews of the principles of CT). In this paper the term 'CT scan' is used to refer to the digital data and image of one slice, but the term is sometimes also used to indicate a full CT examination or a series of images (as in 'to do a CT scan of a specimen').

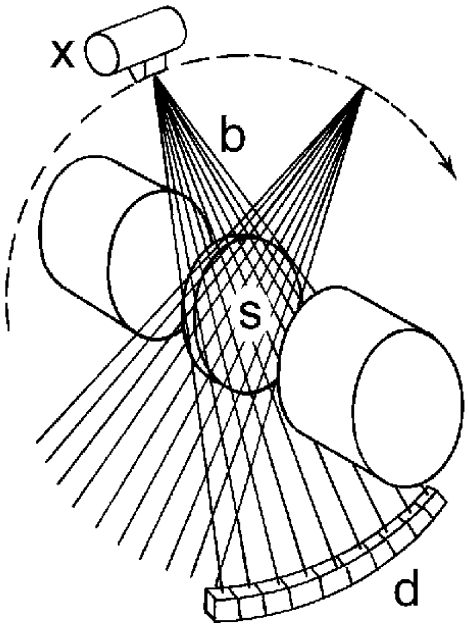

Fig. 2. Diagram showing the principals of data acquisition in CT. The x-ray source (x) and the array of detectors (d) rotate about the specimen and measure its attenuation within the confines of a slice-shaped volume (s) in a great number of directions using a fan beam (b).

In 'spiral' or 'helical' CT, a variant introduced in 1989, the x-ray source and detectors continuously circle the specimen while the table is simultaneously translated. Consequently, the attenuation measurements are taken in a spiral trajectory, rather than as individual slices at fixed table positions. Cross-sectional images can be reconstructed at any given position by means of interpolating these spiral measurements. Spiral CT has important advantages in certain clinical applications. However, these are not relevant when scanning scientific specimens, and the interpolation process necessary to reconstruct planar images from spiral data reduces image quality (Wilting & Zonneveld, 1997; Wilting & Timmer, 1999).

Using cross-sectional images produced by CT overcomes the problems caused by the superimposition of structures in conventional radiographs, and thus provides detailed anatomical information without interference from structures lying on either side of the plane of interest (compare Fig. 1*a*, *b*). Moreover, there is no parallax distortion because the object's density is measured in multiple directions. The spatial resolution of CT is not as good as that of conventional radiography, but it has a better contrast resolution. Its particular relevance for palaeontology is that CT can thus resolve small density differences between fossilised bone and attached rock matrix.

The best possible spatial resolution in the plane of a CT scan that can be achieved with current medical CT scanners is about 0.3–0.5 mm. It is mainly determined by the geometry of the x-ray beam. However, the resolution that is actually obtained may not be as good, because CT scans, like any digital image, are composed of an array of a limited number of 'picture' elements or pixels (Fig. 3). If the fixed image matrix of pixels covers a large area (field of view: FOV), the pixel size is relatively large and this will limit the spatial resolution (Blumenfeld & Glover, 1981). For example, a typical CT scan with a matrix size of 512×512 pixels and a FOV of 240×240 mm has a pixel size of 0.47 mm, and such an image will obviously not have a resolution of 0.3–0.5 mm. This can only be achieved by selecting a smaller FOV to reduce the pixel size (see Spoor et al. 2000 for more details).

Spatial resolution of medical scanners perpendicular to the scan plane is significantly poorer than in the scan plane itself because each CT slice has a thickness that well exceeds the pixel size (minimum slice thickness currently available 0.5–1.5 mm). Thus, each

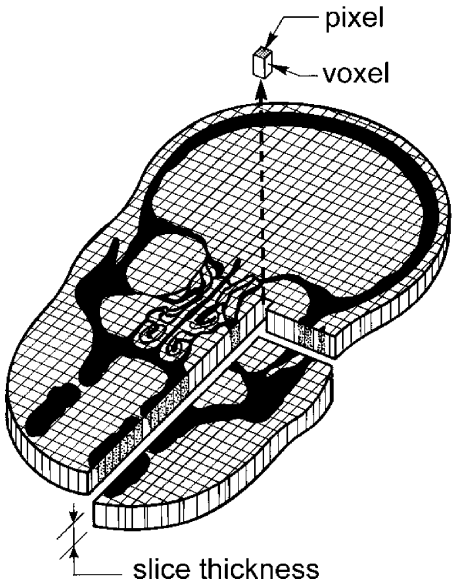

Fig. 3. Diagram of a CT or MR scan with a given slice thickness, demonstrating the concept of the 2-D picture elements, or 'pixels', and their associated volume elements, or 'voxels' (after Zonneveld, 1987).

pixel represents a volume element or voxel (Fig. 3), and the CT number assigned to each pixel is a measure of the average density, the attenuation coefficient, in the voxel. Density differences within a voxel cannot be visualised, a phenomenon known as 'partial volume averaging'.

Dedicated micro-CT scanners can provide images with a much higher 'in-plane' spatial resolution and with a thinner slice thickness than medical CT scanners (see e.g. Flannery et al. 1987; Holdsworth et al. 1993; Anderson et al. 1994; Bonse, 1997; Denison et al. 1997; Illerhaus et al. 1997). Many of these scanners differ from medical ones in that it is the specimen that rotates, rather than the source/detector system. Some are like medical scanners in that cross-sectional images are calculated using attenuation measurements taken from a line of detectors. Others calculate a 3-D volume of CT numbers from radiographs recorded in multiple directions using an image-intensifier and a framegrabber. Cross-sectional images in any direction can be calculated from the data volume. The drawback of the latter method is that the limited dynamic range (latitude) of most image intensifiers means that relatively small contrasts cannot be reproduced accurately in the image reconstruction. Consequently, such systems are less useful for scanning matrix-filled fossils with little contrast between the matrix and the mineralised bone. The in-plane spatial resolution and the slice thickness that can be obtained with micro-CT varies between 1 and about 200 μm, and depends on the size of the specimen. Unlike medical scanners, many of these microtomographs produce isometric voxels, i.e. the pixel size is identical to the slice thickness. Whereas the scan time per slice is in the order of seconds with a medical scanner, it is typically minutes with micro-CT.

In both medical CT and micro-CT the contrast resolution follows from the CT number scale in Hounsfield units (H) on which the attenuation coefficients, calculated for each voxel, are expressed. In medical scanners this scale has typically 4096 units defined by a value of –1000 H for air, and 0 H for water, with very dense tissue, such as dental enamel, close to the maximum value of 3095 H. For display on a computer monitor the 4096 units CT number scale is converted into a 256 units grey scale, enabling the viewer to see tissues with widely-different densities, or to focus on small and specific density differences between tissues (a so-called 'window' technique).

CT scanning skeletal morphology

Given its properties, CT is an ideal modality to examine extant and fossil skeletal morphology, and scans have been used in numerous paleoanthropological and comparative primatological studies to assess, among others, midline cranial architecture (Maier & Nkini, 1984; Ross & Henneberg, 1995; Spoor, 1997; Lieberman, 1998; Spoor et al. 1999), the endocranial cavity (Zonneveld et al. 1989; Conroy et al. 1990), the structure of the cranial vault (Hublin, 1989; Garcia, 1995; Spoor et al. 1998), the paranasal sinuses and both the middle and inner ear (Wind, 1984; Zonneveld & Wind, 1985; Zonneveld et al. 1989; Montgomery et al. 1994; Spoor & Zonneveld, 1994, 1995, 1998; Spoor et al. 1994; Hublin et al. 1996), the dentition (Ward et al. 1982; Conroy & Vannier, 1987, 1991*a*, *b*; Conroy, 1988; Macho & Thackeray, 1992; Bromage et al. 1995; Conroy et al. 1995; Schwartz et al. 1998), cortical bone geometry of the mandible (Demes et al. 1990; Daegling & Grine, 1991; Schwartz & Conroy, 1996), and of long bones (Jungers & Minns, 1979; Tate & Cann, 1982; Senut, 1985; Ruff & Leo, 1986; Ruff, 1989; Ohman et al. 1997). In all of these studies individual 2-D CT images are analysed, but increasingly a stack of contiguous CT scans covering all or part of a specimen is being used as the basis for 3-D imaging, an application that will be discussed below.

In most respects the protocol for CT scanning skeletal specimens is similar to that for clinical use. The most appropriate scan plane and field of view of the scans must be selected so that the relevant morphology is imaged with the best possible spatial

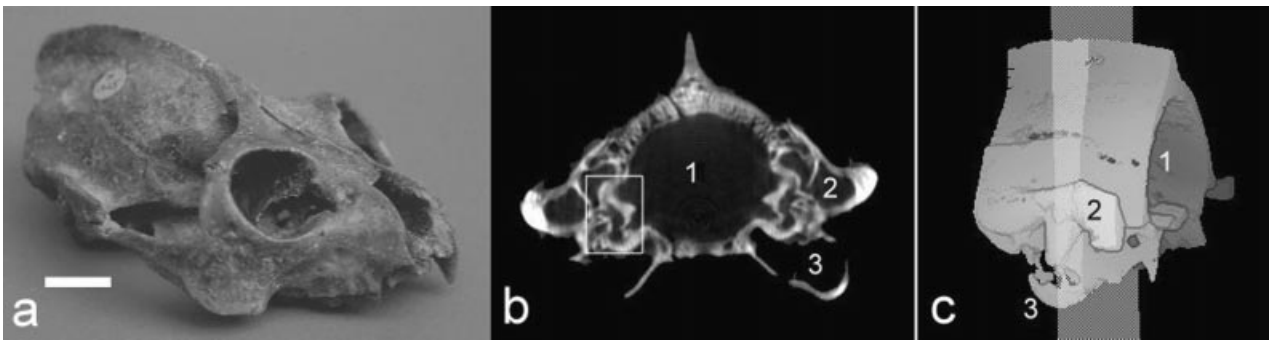

Fig. 4. (*a*) Cranium of *Adapis parisiensis* BM(NH) M1345. Bar, 10 mm. (*b*) Coronal micro-CT scan at the level of the ear region (posterior view; slice thickness 167 µm), showing: 1, the cranial cavity; 2, the root of the zygomatic arch; 3, the right bulla, and aspects of the bony labyrinths (on left side in frame). (*c*) 3-D image showing part of the neurocranial region, with the position of the coronal scan indicated. Numbers as in *b*.

resolution. The choice of scan plane when scanning skeletal specimens is far less restricted than in clinical practice where the possible range of planes is determined by the limitations of the living human body. Another distinction is that clinical radiologists visualising skeletal structures tend to use specific 'bone' filters or kernels for the reconstruction of the images, which are less appropriate for basic morphological research. Such so-called edge-enhancement filters provide images which appear crisper, but the artificial enhancement of interface contrast results in inaccuracies when analysed quantitatively (Spoor, 1993). Neutral filters, such as those used for scanning the abdomen, are therefore more useful as these give the most truthful representation of the boundaries of structures (see Spoor et al. [2000] for further details). When dealing with highly-mineralised and/or matrix-filled fossils CT scans made with regular medical scanners may show a significantly reduced image quality in the form of, for example, streaks or high noise levels. The main reasons are that the fossil's density or overall mass may be outside the normal range found in patients for which the scanner is designed. The most common scanning artefacts in CT images of fossils and possible ways to avoid them are discussed in Zonneveld & Wind (1985), Zonneveld et al. (1989), Spoor & Zonneveld (1994), and in detail in Spoor et al. (2000).

Micro-CT has predominantly been developed for material research or to assess small tissue samples, for example to study mineral content or trabecular structure of bone (Flannery et al. 1987; Kuhn et al. 1990; Anderson et al. 1994, 1996; Müller et al. 1994; Davis & Wong, 1996; Rüegsegger et al. 1996). However, it has also been used successfully to visualise the detailed morphology of extant and fossil crania (Rowe et al. 1993, 1997; Shibata & Nagano, 1996; Thompson & Illerhaus, 1998; Spoor et al. 1998; Spoor & Zonneveld, 1998). An example of a coronal micro-CT slice of an *Adapis* cranium is shown in Figure 4*b*.

MAGNETIC RESONANCE IMAGING (MRI)

MRI was developed in the 1970s (Lauterbur, 1973; Mansfield et al. 1976; Mansfield & Pykett, 1978), on the basis of techniques and principles developed for chemical nuclear magnetic resonance (NMR) spectroscopy, and was later applied in diagnostic imaging as a noninvasive imaging modality (Edelstein et al. 1980).

MRI can produce cross-sectional images or volumetric datasets, using pulses of radiofrequency (RF) energy to map the relative abundance and other physical characteristics of hydrogen nuclei (protons). Before image data can be collected, the protons are aligned into a state of equilibrium by a strong, static magnetic field, their spin axes precessing with a specific frequency about the axis of the field. Using a sequence of RF pulses the spin axes are 'flipped' out of alignment into a higher energy, more excited, state. After the pulses cease, the protons begin to relax back to their original, unexcited, state and in doing so emit energy equivalent to the difference between the 2 energy states. This energy, referred to as the MR signal, or the 'echo', is picked up by a coil, analogous to a TV aerial. The signal intensity depends on the local proton concentration and the chemical environment of the protons. The MR signal intensities are mapped into a 2-D plane, or occasionally a 3-D block, using embedded spatial encoding information. As in CT, the signal calculated for each voxel and its associated pixel are displayed on a computer monitor, using a grey scale with black representing the lowest and white the highest intensity.

Images are usually reconstructed using information from 2 different relaxation processes, known as 'T1' and 'T2'. In T1-weighted images, fat gives a more

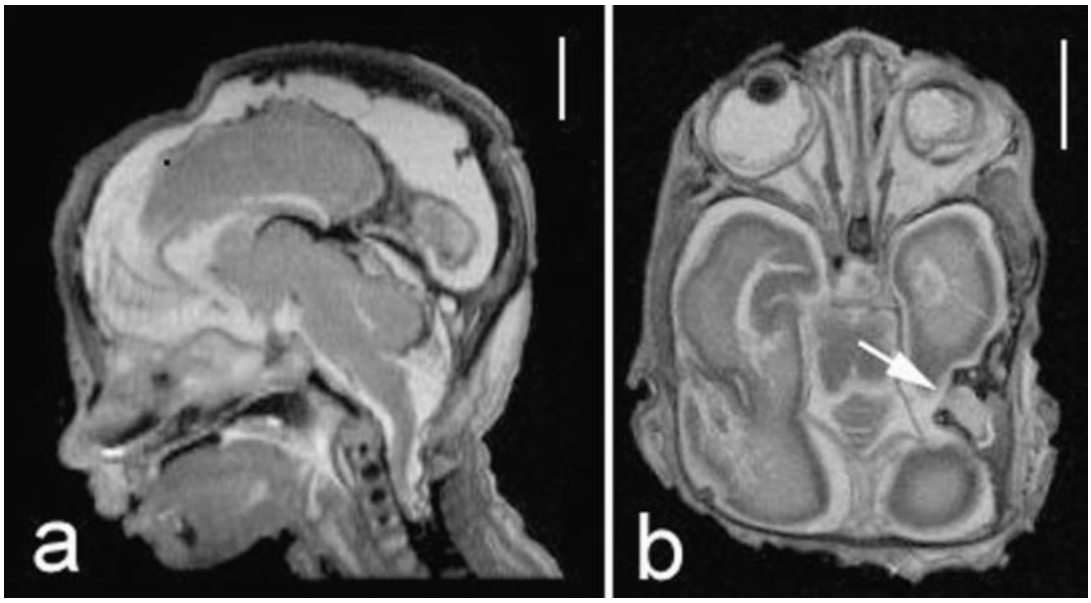

Fig. 5. T2 weighted hrMR images obtained with a 4.7 Tesla field scanner. (*a*) Midsagittal image of a 25 wk-old human fetus (slice thickness 625 μm), showing details of the developing cranial base and brain. (*b*) Transverse image of a fetal mandrill (slice thickness 500 μm), showing the dura-covered opening of the subarcuate fossa (arrow). Bars, 10 mm.

intense signal than water and thus appears brighter, whereas T2-weighted images show the reverse pattern. Since the concentration of fat and water varies between different tissues, it is relatively straightforward to differentiate tissues with sufficient protons by their echoes (Bottomley et al. 1984). In contrast to soft tissues mineralised bone is proton deficient, produces very little echo and thus appears as a signal void in the image. Nevertheless, it is possible to see most, if not all, of the ossified architecture of the skeleton silhouetted against the signal from proton-rich tissues. More detailed accounts of the principles of MRI can be found in Foster & Hutchinson (1987), Bushong (1988), Young (1988), Newhouse & Weiner (1991) and Westbrook & Kaut (1993).

Most clinical MRI units are designed to image adult human morphology, providing in-plane spatial resolutions in the region of 0.7–1 mm, and a slice thickness of about 1–3 mm. These units are therefore not suitable for imaging smaller specimens or for the study of detailed morphology, as encountered in studies of, for example, fetal development, or smaller primate species. Such specimens are best investigated with high-resolution MRI (hrMRI) in which in-plane spatial resolutions in the region of 156–300 μm and slice thicknesses of 300–600 μm are obtained by the use of significantly stronger magnetic fields than in medical MRI (Effman & Johnson, 1988; Johnson et al. 1993; Smith et al. 1994; Smith, 1999). A limitation, as with micro-CT, is that high-resolution MRI requires long imaging times (typically 24 h per specimen).

Applications of MRI in evolutionary studies

The investigation of the comparative and functional aspects of the soft-tissue structures associated with skeletal morphology provide an important foundation for the interpretation of fossil evidence. Likewise, assessing patterns of ontogenetic development of the skeletal system may provide the key to understanding mechanisms of phylogenetic change. In this light, CT and MRI should be seen as complementary techniques in evolutionary studies. Whereas CT provides excellent visualisation of hard tissues in extant and fossil specimens, MRI is the technique of choice to investigate soft-tissues and the ontogeny of the skeleton. For example, phylogenetic changes in brain development have been proposed as one of the major factors underlying cranial morphology (e.g. Ross & Ravosa, 1993; Ross & Henneberg, 1995; Spoor, 1997 and studies cited therein). MRI provides detailed visualisation of both the brain and the cartilaginous cranial base, whereas CT has difficulty distinguishing between brain tissue and the surrounding cerebrospinal fluid (Zonneveld & Fukuta, 1994). Thus, clinical MRI can be used to study adult brain morphology (e.g. Falk et al. 1991; Semendeferi et al. 1997; Rilling & Insel, 1999; Semendeferi & Damasio, 2000), whereas hrMR studies allow the interactions between the brain and the cranium during ontogenetic development to be assessed (Fig. 5*a*; Jeffery & Spoor, 1999). Another example concerns the relationship between the subarcuate fossa in the petrous temporal bone and the petrosal lobule of the cerebellar

paraflocculus. A lobule-bearing fossa is known as a common feature of primates other than humans and great apes (Gannon et al. 1988), but it has been observed that in some large cercopithecids, *Mandrillus* in particular, the fossa tends to be obliterated (Spoor & Leakey, 1996). The hrMR image of a fetal *Mandrillus* specimen demonstrates that its subarcuate fossa is empty and covered by dura (Fig. 5*b*), a morphology similar to that seen in human and great ape fetuses (Gannon et al. 1988).

The practical aspects of obtaining high-quality MR images of particular morphological areas in specimens with different types of preservation is considerably more complex than is the case with CT, because a larger number of scanning parameters have to be selected and fine tuned. For example, individual cases may require specially-designed RF pulse sequences in order to achieve a useful result. Detailed discussion of the manipulation of image contrast, and strategies for dealing with a range of image artefacts can be found in Spoor et al. (2000).

THREE-DIMENSIONAL IMAGING

Using computer graphics techniques, a series of contiguous or overlapping CT or MR images can be stacked to provide a 3-D data set of the scanned object, that can be analysed and visualised in a variety of ways (see e.g. Robb, 1995, for a general overview). This technique is now commonly applied in medical practice (Höhne et al. 1990; Hemmy et al. 1994; Zonneveld, 1994; Zonneveld & Fukuta, 1994; Linney & Alusi, 1998; Ter Haar Romeny et al. 1998; Udupa & Herman, 1998), and is being introduced into paleoanthropology (see e.g. Zollikofer et al. 1998; Spoor & Zonneveld, 1999, for reviews).

Multiplanar reformatting

A 3-D data set enables multiplanar reformatting, i.e. the extraction of images in planes other than the original stack. For example, the midsagittal image of the human fetus shown in Figure 5*a* is resampled from an original stack of transverse hrMR scans. The spatial resolution of reformatted images is not as good as in the original ones, unless the voxels of the image stack are isometric (i.e. the pixel size equals the slice thickness) and the new image is exactly perpendicular to the original image plane. Thus, if the best possible spatial resolution is to be achieved, in particular with a nonisometric data set, it is important to choose the most appropriate plane when making the initial scans, rather than to rely on reformatted images.

3-D visualisation by surface rendering

The second application of 3-D data sets is to obtain reconstructions of all, or selected parts, of a specimen. Even for those experienced in the interpretion of the cross-sectional shapes shown in individual CT or MR scans, 3-D reconstructions provide a much better and more realistic impression of the overall morphology. Usually the reconstructions are based on either CT or MR data sets, but in so-called multimodality-matching different data sets are combined, for example visualising the cranium based on CT, and the brain using MRI (Gamboa-Aldeco et al. 1986; Zuiderveld et al. 1996; Ter Haar Romeny et al. 1998).

In studies of skeletal morphology the most common technique of visualising the 3-D dataset is surface rendering, in which surfaces of selected tissues are extracted from the data volume and imaged. It involves 3 steps. The first, known as segmentation, is the isolation of the tissue, or material, to be imaged in the 3-D reconstruction. This process is performed separately in each CT or MR slice, most commonly by thresholding for the range of CT or MR numbers characterising the relevant tissue. Segmentation can be improved by manually drawing regions of interest, excluding specific parts from the 3-D reconstruction, and by using specialised 'region growing' and 'edge detection' software tools. In the second step the border lines of the selected tissues in each slice are interpolated to create a smooth 3-D surface description of the structure to be imaged. The last step is the illumination of this surface by means of one or more virtual light sources, to emphasise its 3-dimensionality and to bring out surface details. Examples of surface-rendered reconstructions based on regular CT scans and micro-CT scans are shown in Figures 6 and 4*c*, respectively.

Internal structures can be demonstrated in 3-D image reconstructions by making cut-away views in which part of the selected tissue is left out, for example in order to demonstrate the paranasal sinuses, or the endocranial cavity. Visualisation of hollow structures can be improved if they are representated as solid objects ('flood-filling'; Fig. 6). When dealing with reconstructions of soft-tissue specimens cut-away views can be shown with multiplanar-reformatted images mapped onto the cut surfaces. The 3-D effect of reconstructions can be enhanced by generating stereopairs of images, and animation sequences can simulate movement. A particularly appealing method of presenting surface-rendered 3-D reconstructions is through stereolithography which provides life-sized, or enlarged, plastic models that can be handled

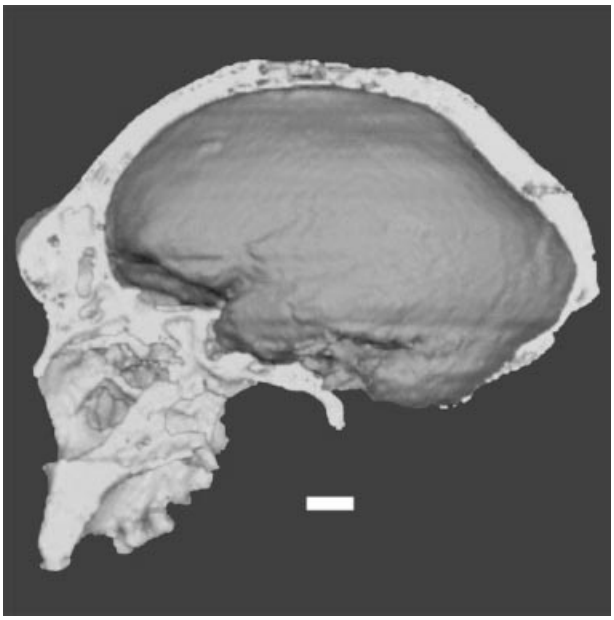

Fig. 6. Surface rendered 3-D image of the Broken Hill specimen, based on 1.5 mm thick CT slices. Cut-away view of the left lateral half reveals the flood-filled endocast. Bars, 10 mm.

manually (Zonneveld, 1994; Zollikofer & Ponce de Leon, 1995; Zollikofer et al. 1995, 1998; Seidler et al. 1997).

Developments on the computer graphics side of 3-D reconstruction have resulted in increasingly realistic images. However, improved visual representation of, for example, the surface of a cranium, does not mean that the image itself is any more accurate. The extent to which the reconstruction reflects reality primarily depends on limitations inherent to CT or MRI. The accuracy of 3-D reconstructions is limited by the spatial resolution within the scan plane and by the slice thickness and slice increment in the direction perpendicular to the scan plane (Vannier et al. 1985). However, the original voxel size may not always be obvious from the final 3-D reconstruction because sophisticated interpolation algorithms lead to excellent smoothing of the steps between the stacked slices.

An important influence on the accuracy of surface-rendered reconstructions is the segmentation process. Software packages for 3-D visualisation most commonly select each structure to be shown by thresholding for a single range of CT or MR numbers characterising the relevant material. A major problem with thresholding in MR images is that different tissues may give MR signals in overlapping ranges. Consequently, surface rendering is less frequently used in MRI-based 3-D reconstruction other than for images showing the skin surface in combination with cut-away views revealing the internal morphology on the cut surfaces.

In CT-based reconstructions a major source of segmentation artefacts is partial volume averaging, the effect that different densities within a voxel are averaged and represented by a single CT number. Thus, the CT numbers of thin bony walls will tend to drop below the segmentation range set for bone because the bone density is averaged with that of surrounding air (Fig. 7), causing artificial holes in 3-D bone reconstructions, that have been referred to as 'pseudoforamina' (Hemmy & Tessier, 1985). Partial volume averaging at the thin edge of bones may also result in reconstructions with sutures that appear too wide, and foramina that appear too large. In fossils the voxels on the interface between dense rock matrix

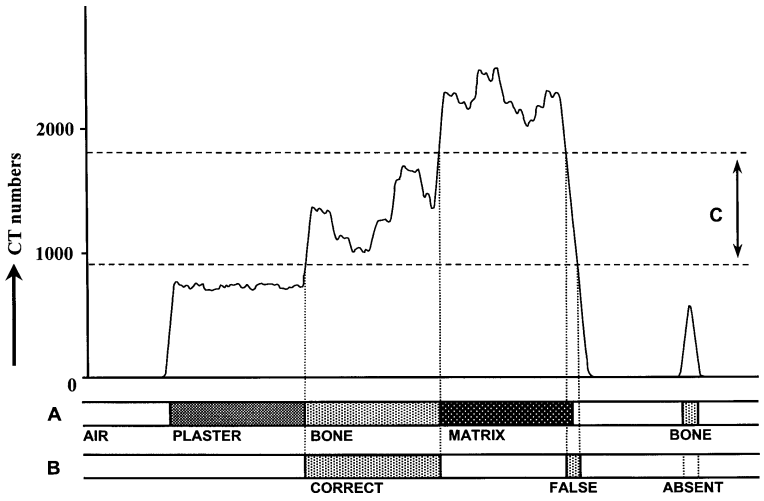

Fig. 7. Graph of CT numbers representing air, plaster, bone, and matrix as indicated in bar 'A'. Bar 'B' shows the effect of partial volume averaging on bone segmentation when thresholding for range 'C'. Pixels at the matrix-air interface have CT numbers in the range of bone, and are therefore incorrectly included in the bone segmentation. Pixels of a thin bony wall on the right are outside the selected range of bone CT numbers and are therefore excluded from the bone segmentation.

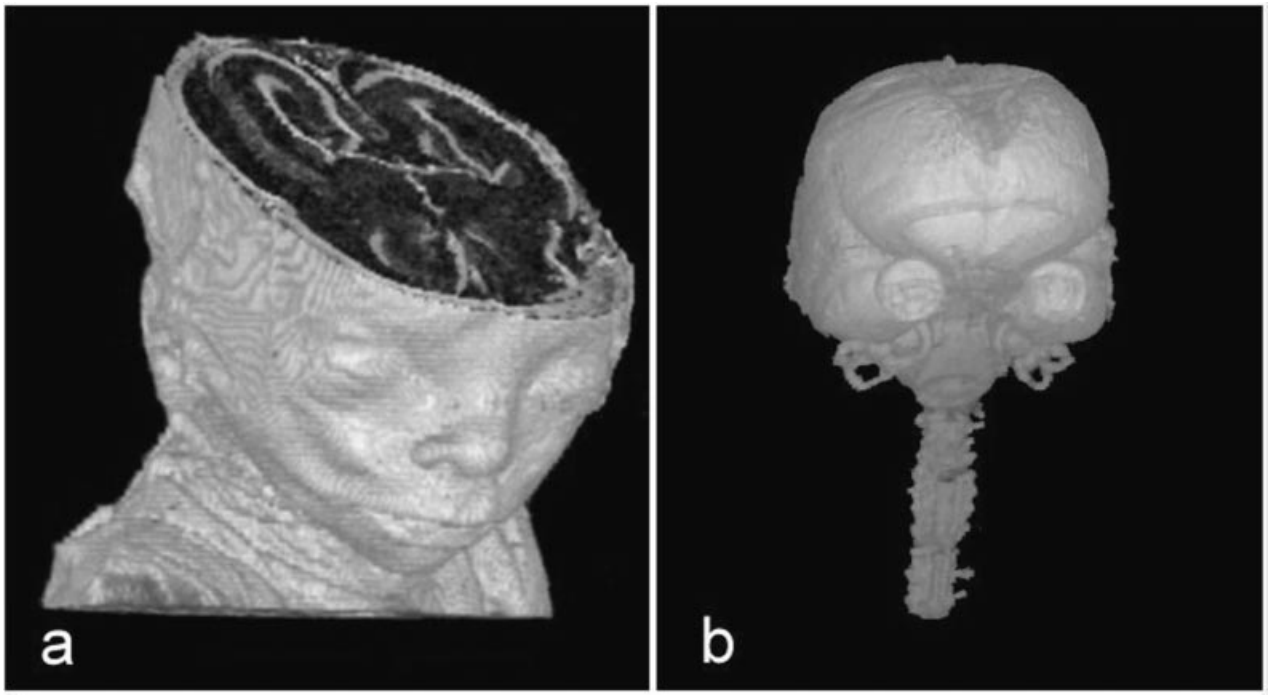

Fig. 8. Volume rendered 3-D images based on the high-resolution MRI dataset of the 25 wk-old fetus shown in Figure 5 *c*. (*a*) Three-quarter frontal view, with the highest opacity assigned to the skin and the top of the head removed to demonstrate the brain morphology. (*b*) Lateral view, with the skin made transparant to demonstrate the outline of the brain, spinal cord, the inner ears and eyes.

and air have intermediate CT numbers which are often in the range of fossil bone, and that will thus be included in bone segmentations (Fig. 7). The segmentation of fossil bone by thresholding is further complicated by local differences in mineralisation and matrix penetration of the bone, and by matrix that locally may have a similar density as bone. Segmentation artefacts can be reduced by manually excluding or including certain areas. To avoid the problems associated with thresholding for a preselected CT number range, so-called 'snake' edge detection techniques have been developed that locally compare the CT numbers on either side of a gradient and select the most likely position of the tissue interface (Gourdon, 1995; Lobregt & Viergever, 1995; McInerney & Terzolpoulos, 1995).

3-D visualisation by volume rendering

An alternative technique of representing 3-D data sets is volume rendering, in which all of the data volume contributes to the images (Levoy, 1988; Drebin et al. 1988; Toga, 1990; Robb, 1995). Tissue segmentation, the crucial step in surface rendering, is therefore skipped, unless it is used to isolate the structure that is to be volume-rendered. Different CT or MR numbers in the stack of slices are assigned different colours and different degrees of opacity. Subsequently, this volume description is projected onto a plane for viewing. For example, in Figure 8 voxels representing either skin or brain tissue have been given an opacity higher than those representing other tissues.

Volume rendering and surface rendering techniques both have their strong and weak points, and the choice of technique depends on the requirements of the study (Rusinek et al. 1991; Udupa et al. 1991). Volume rendering has the advantage that many aspects of the internal and external morphology of a specimen can be shown in relation to each other without the need for a laborious segmentation process and complicated cut-away views. It is especially useful where tissue segmentation is problematic or impractical, as in MRI. However, the computational cost of volume rendering is high, requiring more time than surface rendering. Moreover, the fuzzy representation of surfaces and some degree of superimposition of structures that characterise volume rendering make surface rendering the more appropriate technique to reconstruct skeletal morphology.

3-D visualisation and human evolutionary studies

Three-dimensional imaging based on CT has been applied in paleoanthropological studies and comparative primatological analyses in order to assess,

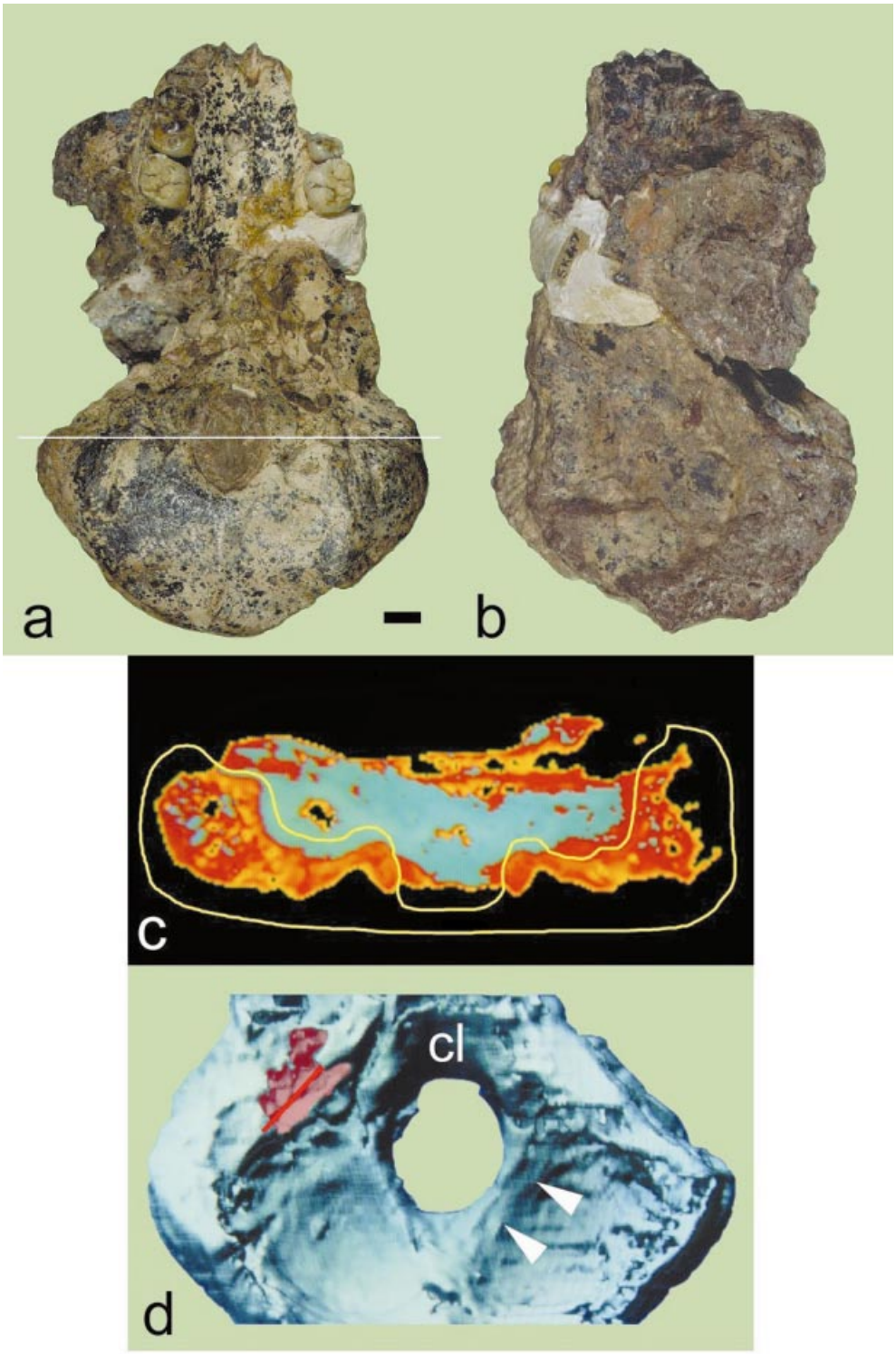

Fig. 9. Imaging the *Australopithecus robustus* partial cranium SK 47. (*a*) Basal view (scale bar is 10 mm). (*b*) Superior view. (*c*) Coronal CT scan at the level of the foramen magnum as indicated by the line in *a* (slice thickness 1.5 mm). Pixels with CT numbers in the range selected for the segmentation of bone are represented in a colour scale, the others in a grey scale. The yellow line is the region of interest (ROI) manually drawn to exclude unwanted areas in the endocranial cavity from the reconstruction. These areas represent bone fragments and matrix with densities in the bone range. (*d*) Superior view of the surface-rendered 3-D reconstruction of the cranial base with the endocranial matrix and bone fragments removed, showing a groove for the right occipital-marginal sinus (arrowheads). The clivus is indicated (cl), and the reddish area marks an artificial hole in the left petrous pyramid (see text). The red line over this area represents the missing superior margin of the left petrous temporal bone (after Spoor & Zonneveld, 1999).

among others, unerupted tooth crowns, dental root morphology, the paranasal sinuses, the inner ear, the endocranial surface, and cranial vault thickness (Zonneveld et al. 1989; Koppe & Schumacher, 1992; Zollikofer et al. 1995, 1998; Koppe et al. 1996; Seidler et al. 1997; Conroy et al. 1998; Thompson & Illerhaus, 1998; Ponce de Leon & Zollikofer, 1999; Spoor & Zonneveld, 1999; Rae & Koppe, 2000). MRI-based 3-D visualisation has been applied in comparative primatological analyses of brain morphology (Semendeferi et al. 1997; Rilling & Insel, 1999; Semendeferi & Damasio, 2000). A second category of applications is the reconstruction of fossils by complementing missing parts through mirror imaging (Zollikofer et al. 1995), or by combining scaled components from more than one individual (Kalvin et al. 1995). The bones of a crushed fossil can be 'electronically dissected' and reassembled, and plastic deformation corrected (Braun, 1996). In a third type of application, 3-D reconstructions are used as the basis for morphometric studies (see next section).

An important application of CT-based 3-D reconstruction in paleoanthropology is the possibility to 'electronically remove' any matrix attached to a specimen. A practical example concerns the *Australopithecus robustus* SK 47 specimen from Swartkrans in southern Africa. This fossil is the only undistorted cranial base of this species currently known (Fig. 9*a*), but its endocranial morphology cannot be studied directly because the cranial cavity is filled with matrix and bone fragments of the crushed cranial vault (Fig. 9*b*). This area is of considerable interest because basicranial features play an important role in the debate over the phylogenetic relationship between species of 'robust' australopithecines and in reports on similarities between these hominins and *Homo* (Dean, 1986, 1988; Grine, 1988; Walker & Leakey, 1988; Strait et al. 1997). To visualise the endocranial surface of SK 47 Spoor & Zonneveld (1999) therefore prepared a surface-rendered 3-D reconstruction without the matrix infill. This proved particularly challenging because the CT numbers of many areas of the infill are within the bone range (Fig. 9*c*). Some of these areas represent actual bone fragments, some are caused by partial volume averaging at matrix-air interfaces, and at some spots the matrix is in the bone range. These areas of the infill were removed manually in each of the 50 CT images (Fig. 9*c*).

The reconstructed SK 47 basicranium is shown in superior view in Figure 9*d*. The irregular hole in the left petrosal surface is a segmentation artefact. The dense otic capsule falls in the CT number range of the matrix, and the thin overlying layer of cortical bone is not shown owing to partial volume averaging. Important aspects of the basicranium that can thus be assessed on the basis of the reconstruction are the orientation of the basioccipital clivus and the petrous pyramids, and the venous sinus pattern that includes a well-developed right occipital-marginal sinus (Fig. 9*d*; see Spoor & Zonneveld, 1999, for further discussion). Clear visualisation of the groove for the occipital-marginal sinus could only be achieved by relocating the virtual light sources so that the reconstructed surface is illuminated by oblique light. The drawback is that the hard shadows make the overall visualisation of the reconstruction less appealing (Fig. 9*d*).

QUANTITATIVE ANALYSIS

CT and MRI can form the basis for morphometric analyses, using either individual scans or 3-D reconstructions to obtain landmark data, linear dimensions, angles, surface areas, or volumes. The accuracy of such measurements depends on the spatial resolution, the pixel or voxel size and on the specific display settings of the image when the measurement is taken. In scans of large structures the accuracy of measurements will be determined by the pixel size of the image and not by the spatial resolution. In this situation boundaries of structures are well-defined and positioning landmarks or drawing area contours is usually no problem. In images with a pixel size sufficiently small not to be the limiting factor the accuracy depends on the spatial resolution. Taking measurements of detailed morphology in such images may be complicated by the fact that structures are unavoidably shown with blurred boundaries, owing to the limited resolution, and that the apparent size of structures changes when the display settings of the image are altered. In many cases the exact position of a boundary can nevertheless be established on the basis of the local CT or MR numbers. Discussion of this approach and of other more technical aspects of measurement accuracy and precision are considered in detail in Hildeboldt et al. (1990), Vannier et al. (1991), Spoor et al. (1993), MacFall et al. (1994); Richtsmeier et al. (1995), Feng et al. (1996) and Ohman et al. (1997).

CT is also used to obtain density measurements of bone and teeth, examining absolute and relative values and their distribution (Genant & Boyd, 1977; Cann & Genant, 1980; Adams et al. 1982; Glüer et al. 1988; Glüer & Genant, 1989; Steenbeek et al. 1992; Anderson et al. 1996). This information can be important when investigating the biomechanical pro-

perties and functional morphology of skeletal structures, but caution is warranted since CT-based densitometry is marked by a range of pitfalls and technical limitations (see discussion in Cann et al. 1979; Newton & Potts, 1981; Ruff & Leo, 1986; Spoor et al. 2000). Density measurements of fossils are particularly problematic because of unknown taphonomic factors. Fossils found in caves are often partially penetrated by calcite with a very high density, whereas air-exposed parts may have been decalcified.

FUTURE PROSPECTS

In the short term, the main advances in the application of CT and MRI in morphological research will be in data processing rather than data acquisition. Driving factors include the opportunities created by the ever-increasing computer power and the demand for fast and life-like 3-D rendering techniques coming from the film industry and advanced medical applications such as surgical simulation and virtual endoscopy. Three-dimensional rendering software will become quicker, easier to use and less expensive as the performance gap between Unix workstations and personal computers narrows further.

For a long time, the manipulation of CT and MR images was confined to the specialist realm of UNIX-based computer environments. This, together with the multitude of brand-specific image formats used to handle these images, made postacquisition image manipulation almost impossible without the help of a medical physicist or software engineer. With the increase in power of personal computers, and the emergence of appropriate software and universal formats, such as DICOM (Digital Imaging and Communications in Medicine), it is now possible to do both basic manipulations and more complex 3-D reconstructions on a PC or Mac. Spoor et al. (2000) describe some basic techniques and suggestions on handling images on computers.

Multimodality matching, combining CT and MRI based 3-D datasets, will become a mainstream technique, and will improve the integration of morphological information that can be extracted from soft-tissue specimens. The use of 3-D datasets as the basis for complex multivariate morphometric studies will increase (O'Higgins & Jones, 1998; O'Higgins, 2000), including the possibility of morphing surface-rendered reconstructions between different taxa and developmental stages.

More widespread application of CT and MRI in comparative, developmental and evolutionary studies is starting to result in extensive scientific image archives that document, for example, hominin fossils and human fetal growth series. The Internet forms the ideal structure to provide worldwide access to such reference collections. The availability of the common DICOM image format, supported by the major medical imaging companies, will further contribute to routine exchange of datasets.

The image quality that can be obtained with medical CT has remained stable over the past decade. What has changed dramatically, however, is the speed of scanning. Faster scanners make the acquisition of 3-D sets of a large number of specimens for a given research project increasingly feasible. Whereas micro-CT used to be experimental and the machines were purpose built, there is a trend towards affordable and commercially-available scanners. Portability will have the consequence that such scanners will increasingly be taken to the specimens in a museum collection.

MRI will see further improvements in image quality through the use of stronger magnets, better coil designs and refined encoding gradients, and faster pulse sequences will shorten imaging times. The potential of MRI for studying skeletal morphology in relation to the associated soft-tissue structures has only recently been realised, and a wide range of applications remains to be explored.

In short, the development of CT and MRI, in combination with powerful computer graphics software, has provided a range of new opportunities to qualitatively and quantitatively study many aspects of human evolutionary history. Following an initial phase during which both researchers and a more general audience marvelled at the capability of these techniques to produce beautiful 2-D and 3-D images, the true scientific value of purposefully-uncovering evidence not accessible by other means has now become abundantly clear.

ACKNOWLEDGEMENTS

We thank the Governors of the National Museums of Kenya, N. Adamali, J. Hooker, P. Kinchesh, R. Kruszynski, D. Kuschel, M. Leakey, P. Liepins, J. Lynch, D. Panagos, D. Plummer, R. Ratnam, B. Sokhi, C. Stringer, J. de Souza, M. Tighe and F. Thackeray for permission and help with scanning the specimens used in the examples. We are grateful to E. Cady, C. Dean A. Linney, J. Moore, G. Schwartz, B. Wood and an anonymous referee for comments. Support from The University of London Intercollegiate Research Service scheme at Queen Mary and Westfield College, The Leakey Foundation, Siemens,

Philips Medical Systems, The Royal Society, the British Council, the UCL Graduate School Fund and the Medical Research Council is acknowledged. This paper is dedicated to the memory of the late Professor Nigel Holder.

REFERENCES

ADAMS JE, CHEN SZ, ADAMS PH, ISHERWOOD I (1982) Measurement of trabecular bone mineral by dual-energy computed tomography. *Journal of Computer Assisted Tomography* **6**, 601–607.

ANDERSON P, DAVIS GR, ELLIOTT JC (1994) Microtomography. *Microscopy and Analysis* March, 31–33.

ANDERSON P, ELLIOTT JC, BOSE U, JONES SJ (1996) A comparison of the mineral content of enamel and dentine in human premolars and enamel pearls measured by X-ray microtomography. *Archives of Oral Biology* **41**, 281–290.

ANGST R (1967) Beitrag zum Formwandel des Craniums der Ponginen. *Zeitschrift für Morphologie und Anthropologie* **58**, 109–151.

BLUMENFELD SM, GLOVER G (1981) Spatial resolution in computed tomography. In *Radiology of the Skull and Brain* (*Vol.* 5)*; Technical Aspects of Computed Tomography* (ed. Newton TH, Potts DG), pp. 3918–3940. St Louis: Mosby.

BONSE U (1997) Developments in X-ray tomography. *SPIE Proceedings* **3149**, 1–264.

BOTTOMLEY PA, FOSTER TH, ARGERSINGER RE, PFEIFER IM (1984) A review of normal tissue hydrogen NMR relaxation times and relaxation mechanisms from 1–100 MHz: dependence on tissue type, NMR frequency, temperature, species, excision and age. *Medical Physics* **11**, 425–448.

BRAUN M (1996) *Applications de la scanographie a RX et de l'imagerie virtuelle en paleontologie humaine*. Paris: PhD Thesis, Museum Nationale d'Histoire Naturelle.

BROMAGE TG, SCHRENK F, ZONNEVELD FW (1995) Paleoanthropology of the Malawi rift — an early hominid mandible from the Chiwondo beds, northern Malawi. *Journal of Human Evolution* **28**, 71–108.

BRÜHL (1896) Über Verwendung von Röntgenschen X-Strahlen zu paläontologisch-diagnostischen Zwecken. *Archiv für Anatomie und Physiologie* 547–550.

BUSHONG SC (1988) *Magnetic Resonance Imaging*, *Physical and Biological Principles*. St Louis: Mosby.

CANN CE, GENANT HK, BOYD DP (1979) Precise measurement of vertebral mineral in serial studies using CT. *Journal of Computer Assisted Tomography* **3**, 852–853.

CANN CE, GENANT HK (1980) Precise measurement of vertebral mineral content using computed tomography. *Journal of Computer Assisted Tomography* **4**, 493–500.

CONROY GC (1988) Alleged synapomorphy of the M1/I1 eruption pattern in robust Australopithicines and *Homo*: evidence from high-resolution computed tomography. *American Journal of Physical Anthropology* **75**, 487–492.

CONROY GC, VANNIER MW (1987) Dental development of the Taung skull from computerized tomography. *Nature* **329**, 625–627.

CONROY GC, VANNIER MW, TOBIAS PV (1990) Endocranial features of *Australopithecus africanus* revealed by 2- and 3-D computed tomography. *Science* **247**, 838–841.

CONROY GC, VANNIER MW (1991*a*) Dental development in South African australopithecines. Part I: problems of pattern and chronology. *American Journal of Physical Anthropology* **86**, 121–136.

CONROY GC, VANNIER MW (1991*b*) Dental development in South African australopithecines. Part II: dental stage assessment. *American Journal of Physical Anthropology* **86**, 137–156.

CONROY GC, LICHTMAN JW, MARTIN LB (1995) Some observations on enamel thickness and enamel prism packing in the Miocene hominoid *Otavipithecus namibiensis*. *American Journal of Physical Anthropology* **98**, 595–600.

CONROY GC, WEBER GW, SEIDLER H, TOBIAS PV, KANE A, BRUNSDEN B (1998) Endocranial capacity in an early hominid cranium from Sterkfontein, South Africa. *Science* **280**, 1730–1731.

CRAMER DL (1977) Craniofacial morphology of *Pan paniscus*. A morphometric and evolutionary appraisal. *Contributions to Primatology* **10**. Basel: Karger.

DAEGLING DJ, GRINE FE (1991) Compact bone distribution and biomechanics of early hominid mandibles. *American Journal of Physical Anthropology* **86**, 321–339.

DAVIS GR, WONG FS (1996) X-ray microtomography of bones and teeth. *Physiological Measurement* **17**, 121–146.

DEAN MC (1986) *Homo* and *Paranthropus*: similarities in the cranial base and developing dentition. In *Major Topics in Primate and Human Evolution* (ed. Wood B, Martin L, Andrews P), pp. 249–265. Cambridge: Cambridge University Press.

DEAN MC (1988) Growth processes in the cranial base of hominoids and their bearing on morphological similarities that exist in the cranial base of *Homo* and *Paranthropus*. In *Evolutionary History of the* '*Robust*' *Australopithecines* (ed. Grine FE), pp. 107–112. New York: A. de Gruyter.

DEAN MC, WOOD BA (1981) Metrical analysis of the basicranium of extant hominoids and Australopithecus. *American Journal of Physical Anthropology* **54**, 63–71.

DEAN MC, STRINGER CB, BROMAGE TG (1986) Age and death of the Neanderthal child from Devil's tower, Gibraltar and the implications for studies of general growth and development in Neanderthals. *American Journal of Physical Anthropology* **70**, 301–309.

DEMES B, TEPE E, PREUSCHOFT H (1990) Functional adaptations in corpus morphology of neandertal mandibles. *American Journal of Physical Anthropology* **81**, 214.

DENISON C, CARLSON WD, KETCHAM RA (1997) Three-dimensional quantitative textural analysis of metamorphic rocks using high-resolution computed x-ray tomography: Part 1. Methods and techniques. *Journal of Metamorphic Geology* **15**, 29–44.

DMOCH R (1975) Beiträge zum Formenwandel des Primatencraniums mit Bemerkungen zu den Knickungsverhältnissen. IV. *Gegenbauer Morphologisches Jahrbuch* **121**, 625–668.

DMOCH R (1976) Beiträge zum Formenwandel des Primatencraniums mit Bemerkungen zu den Knickungsverhältnissen. V. *Gegenbauer Morphologisches Jahrbuch* **122**, 1–81.

DREBIN RA, CARPENTER L, HANRAHAN P (1988) Volume rendering. *Computer Graphics* **22**, 65–74.

EDELSTEIN WA, HUTCHINSON JMS, JOHNSON G, REDPATH T (1980) Spin warp NMR imaging and applications to human whole-body imaging. *Physics in Medicine and Biology* **25**, 751–756.

EFFMANN EL, JOHNSON GA (1988) Magnetic resonance microscopy of chick embryos *in ovo*. *Teratology* **38**, 59–65.

FALK D, HILDEBOLT C, CHEVERUD J, KOHN LAP, FIGIEL G VANNIER M (1991) Human cortical asymmetries determined with 3D MR technology. *Journal of Neuroscience Methods* **39**, 185–191.

FENART R, EMPEREUR-BUISSON R (1970) Application de la methode 'vestibulaire' d'orientation au crane de l'enfant du Pech-de-l'Aze et comparaison avec d'autres cranes neandertaliens. *Archives d'Institut de Paleontologie Humaine* **33**, 89–104.

FENART R, PELLERIN C (1988) The vestibular orientation method; its application in the determination of an average human skull type. *International Journal of Anthropology* **3**, 223–219.

FENG Z, ZIV I, RHO J (1996) The accuracy of computed

tomography-based linear measurements of human femora and titanium stem. *Investigative Radiology* **31**, 333–337.

FLANNERY BP, DECKMAN HW, ROBERGE WG, D'AMICO KL (1987) Three-dimensional x-ray tomography. *Science* **237**, 1439–1444.

FOSTER MA, HUTCHINSON JMS (1987) *Practical NMR Imaging*. Oxford: IRL Press.

GAMBOA-ALDECO A, FELLINGHAM LL, CHEN GTY (1986) Correlation of 3D surfaces from multiple modalities in medical imaging. *Proceedings SPIE* **626**, 467–473.

GANNON PJ, EDEN AR, LAITMAN JT (1988) The subarcuate fossa and cerebellum of extant primates: comparative study of a skull-brain interface. *American Journal of Physical Anthropology* **77**, 143–164.

GARCIA RA (1995) *Application de la tomographie informatisée et de l'imagerie virtuelle a l'analyse quantitative de la structure des parois craniennes*. Mémoire de DEA, Laboratoire d'Anthropologie, Université de Bordeaux.

GENANT HK, BOYD D (1977) Quantitative bone mineral analysis using dual-energy computed tomography. *Investigative Radiology* **12**, 545–551.

GLÜER C, REISER UJ, DAVIS CA, RUTT BK, GENANT HK (1988) Vertebral mineral determination by quantitative computed tomography (QCT): accuracy of single and dual energy measurements. *Journal of Computer Assisted Tomography* **12**, 242–258.

GLÜER CC, GENANT HK (1989) Impact of marrow fat on accuracy of quantitative CT. *Journal of Computer Assisted Tomography* **13**, 1023–1035.

GORJANOVIC-KRAMBERGER K (1906) *Der diluviale Mensch von Krapina in Kroatien*. Wiesbaden: Kriedel.

GOURDON A (1995) Simplification of irregular surfaces meshes in 3D medical images. In *Computer Vision, Virtual Reality and Robotics in Medicine* (ed. Ayache N), pp. 413–419. Berlin: Springer.

GRINE FE (1988) Evolutionary history of the "robust" australopithecines: a summary and historical perspective. In *Evolutionary History of the "Robust" Australopithecines* (ed. Grine FE), pp. 509–520. New York: A. de Gruyter.

HEMMY DC, TESSIER PL (1985) CT of dry skulls with craniofacial deformities: accuracy of three-dimensional reconstruction. *Radiology* **157**, 113–116.

HEMMY DC, ZONNEVELD FW, LOBREGT S, FUKUTA K (1994) A decade of clinical three-dimensional imaging: a review. Part I. Historical development. *Investigative Radiology* **29**, 489–496.

HILDEBOLT CF, VANNIER MW, KNAPP RH (1990) Validation study of skull three-dimensional computerized tomography measurements. *American Journal of Physical Anthropology* **82**, 283–294.

HÖHNE KH, FUCHS H, PIZER SM (1990) 3*D Imaging in Medicine*. NATO ASI Series F: Computer and Systems Sciences, **60**. Berlin: Springer.

HOLDSWORTH DW, DRANGOVA M, FENSTER A (1993) A high-resolution XRII-based quantitative volume CT scanner. *Medical Physics* **20**, 449–462.

HOTTON F, KLEINER S, BOLLAERT A, TWIESSELMAN F (1976) Le rôcher des Neanderthaliens de Spy, étude radio-anatomique. *Journal Belge de Radiologie* **59**, 39–50.

HOUNSFIELD GN (1973) Computerized transverse axial scanning (tomography): Part 1. Description of system. *British Journal of Radiology* **46**, 1016–1022.

HUBLIN J-J (1989) Les characteres dérivés d'*Homo erectus*: rélation avec augmentation de la masse squelettique. In *Hominidae* (ed. Giacobini G), pp. 199–204. Milan: Jaca Books.

HUBLIN J-J, SPOOR F, BRAUN M, ZONNEVELD F, CONDEMI S (1996) A late Neanderthal from Arcy-sur-Cure associated with Upper Palaeolithic artefacts. *Nature* **381**, 224–226.

ILLERHAUS B, GOEBBELS J, RIESEMEIER H (1997) Computerized tomography — synergism between technique and art. In : *Selected Contributions to the International Conference on New Technologies in the Humanities, and Fourth International Conference on Optics within Life Sciences* (ed. Dirksen D, Von Bally G), pp. 91–104. Heidelberg: Springer.

JEFFERY N, SPOOR F (1999) Human fetal cranial base flexion and brain volumes: a high resolution Magnetic Resonance Imaging (hrMRI) study. *American Journal of Physical Anthropology, Supplement* **28**, 161.

JOHNSON GA, BENVENISTE H, BLACK RD, HEDLUND LW, MARONPOT RR, SMITH BR (1993) Histology by magnetic resonance microscopy. *Magnetic Resonance Quarterly* **9**, 1–30.

JUNGERS WL, MINNS RJ (1979) Computed tomography and biomechanical analysis of fossil long bones. *American Journal Physical Anthropology* **50**, 285–290.

KALVIN AD, DEAN D, HUBLIN J-J (1995) Reconstruction of human fossils. *IEEE Computer Graphics and Applications* **15**, 12–15.

KOPPE T, SCHUMACHER K-U (1992) Untersuchungen zum Pneumatisationsgrad des Viscerocranium beim Menschen und bei den Pongiden. *Acta Anatomica Nippon* **67**, 725–734.

KOPPE T, INOUE Y, HIRAKI Y, NAGAI H (1996) The pneumatization of the facial skeleton in the Japanese macaque (*Macaca fuscata*) – a study based on computerized three-dimensional reconstructions. *Anthropological Sciences* **104**, 31–41.

KUHN JL, GOLDSTEIN SA, FELDKAMP LA, GOULET RW, JESION G (1990) Evaluation of a microcomputed tomography system to study trabecular bone structure. *Journal of Orthopedic Research* **8**, 833–842.

LAUTERBUR PC (1973) Image formation by induced local interactions: examples employing nuclear magnetic resonance. *Nature* **242**, 190–191.

LEVOY M (1988) Display of surfaces from volume data. *IEEE Computer Graphics and Applications* May, 29–37.

LIEBERMAN D (1998) Sphenoid shortening and the evolution of modern human cranial shape. *Nature* **393**, 158–162.

LIEBERMAN D, McCARTHY R (1999) The ontogeny of cranial base angulation in humans and chimpanzees and its implications for reconstructing pharyngeal dimensions. *Journal of Human Evolution* **36**, 487–517.

LINNEY AD, ALUSI GH (1998) Clinical applications of computer aided visualization. *Journal of Visualization* **1**, 95–109.

LOBREGT S, VIERGEVER MA (1995) A discrete dynamic contour model. *IEEE Transactions on Medical Imaging* **14**, 12–24.

MACCHIARELLI R, BONDIOLI L, GALICHON V, TOBIAS PV (1999) Hip bone trabecular architecture shows uniquely distinctive locomotor behaviour in South African australopithecines. *Journal of Human Evolution* **36**, 211–232.

MACFALL JR, BYRUM CE, PARASHOS I, EARLY B, CHARLES HC, CHITTILLA V et al. (1994) Relative accuracy and reproducibility of regional MRI brain volumes for point-counting methods. *Psychiatry Research* **55**, 167–177.

MACHO GA, THACKERAY JF (1992) Computed tomography and enamel thickness of maxillary molars of Plio-Pleistocene hominids from Sterkfontein, Swartkrans and Kromdraai (South Africa): an exploratory study. *American Journal of Physical Anthropology* **89**, 133–143.

MAIER W, NKINI A (1984) Olduvai Hominid 9: new results of investigation. *Courier Forschungsinstitut Senckenberg* **69**, 123–130.

MANSFIELD P, MAUDSLEY AA, BAINES T (1976) Fast scan proton imaging by NMR. *Journal of Physics, E. Scientific Instruments* **9**, 271–278.

MANSFIELD P, PYKETT IL (1978) Biological and medical imaging by NMR. *Journal of Magnetic Resonance* **29**, 355–373.

McINERNEY T, TERZOLPOULOS D (1995) Medical imaging segmentation using topologically adaptable snakes. In *Computer Vision, Virtual Reality and Robotics in Medicine* (ed. Ayache N), pp. 92–101. Berlin: Springer.

MONTGOMERY PQ, WILLIAMS HOL, READING N, STRINGER CB (1994) An assessment of the temporal bone lesions of the Broken Hill cranium. *Journal of Archaeological Sciences* **21**, 331–337.

MÜLLER R, HILDEBRAND T, RÜEGSEGGER P (1994) Non-invasive bone biopsy: a new method to analyse and display the three-dimensional structure of trabecular bone. *Physics in Medicine and Biology* **39**, 145–164.

NEWHOUSE J, WEINER J (1991) *Understanding MRI*. Boston: Little Brown.

NEWTON TH, POTTS DG (1981) *Radiology of the Skull and Brain* (*vol. 5*)*; Technical Aspects of Computed Tomography*. St Louis: Mosby.

O'HIGGINS P (2000) Quantitative approaches to the study of craniofacial growth and evolution: advances in morphometric techniques. In *Development, Growth and Evolution*: *Implications for the Study of the Hominid Skeleton* (ed. O'Higgins P, Cohn M). London: Academic Press, in press.

O'HIGGINS P, JONES N (1998) Facial growth in *Cercocebus torquatus*: an application of three-dimensional variation. *Journal of Anatomy* **193**, 251–272.

OHMAN JC, KROCHA TJ, LOVEJOY CO, MENSFORTH RP, LATIMER B (1997) Cortical bone distribution in the femoral neck of hominoids: implications for the locomotion of *Australopithecus afarensis*. *American Journal of Physical Anthropology* **104**, 117–131.

PONCE DE LEON MS, ZOLLIKOFER CPE (1999) New evidence from Le Moustier 1: computer-assisted reconstruction and morphometry of the skull. *Anatomical Record* **254**, 474–489.

PRICE JL, MOLLESON TI (1974) A radiographic examination of the left temporal bone of Kabwe man, Broken Hill mine, Zambia. *Journal of Archaeological Sciences* **1**, 285–289.

PUTZ R (1974) Schädelform und Pyramiden. Zur Lage der Pyramiden in der Schädelbasis. *Anatomische Anzeiger* **135**, 252–266.

RAE TC, KOPPE T (2000) Isometric scaling of maxillary sinus volume in hominoids. *Journal of Human Evolution*, in press.

RAVOSA MJ (1988) Browridge development in Cercopithecidae: a test of two models. *American Journal of Physical Anthropology* **76**, 535–555.

RICHTSMEIER JT, PAIK CH, ELFERT PC, COLE TM, DAHLMAN HR (1995) Precision, repeatability, and validation of the localization of cranial landmarks using computed tomography scans. *Cleft Palate-Craniofacial Journal* **32**, 217–227.

RILLING JK, INSEL TR (1999) The primate neocortex in comparative perspective using magnetic resonance imaging. *Journal of Human Evolution* **37**, 191–223.

ROBB RA (1995) *Three-Dimensional Imaging*. New York: VCH.

ROSS CF, RAVOSA MJ (1993) Basicranial flexion, relative brain size, and facial kyphosis in nonhuman primates. *American Journal of Physical Anthropology* **91**, 305–324.

ROSS CF, HENNEBERG M (1995) Basicranial flexion, relative brain size, and facial kyphosis in *Homo sapiens* and some fossil hominids. *American Journal of Physical Anthropology* **98**, 575–593.

ROWE T, CARLSON W, BOTTORFF W (1993) Thrinaxodon, *Digital Atlas of the Skull* (CD-Rom). Austin: University of Texas Press.

ROWE T, KAPPELMAN J, CARLSON WD, KETCHAM RA, DENISON C (1997) High-resolution computed tomography: a breakthrough technology for earth scientists. *Geotimes* **42**, 23–27.

RUFF CB (1989) New approaches to structural evolution of limb bones in primates. *Folia Primatologica* **53**, 142–159.

RUFF CB, LEO FP (1986) Use of computed tomography in skeletal structure research. *Yearbook of Physical Anthropology* **29**, 181–196.

RUNESTAD JA, RUFF CB, NIEH JC, THORINGTON RW, TEAFORD MF (1993) Radiographic estimation of long bone cross-sectional geometric properties. *American Journal of Physical Anthropology* **90**, 207–213.

RUSINEK H, NOZ ME, MAGUIRE CQ, CUTTING C, HADDAD B, KALVIN A et al. (1991) Quantitative and qualitative comparison of volumetric and surface rendering techniques. *IEEE Transactions on Nuclear Science* **38**, 659–662.

RÜEGSEGGER P, KOLLER B, MÜLLER R (1996) A micro-tomographic system for the nondestructive evaluation of bone architecture. *Calcified Tissue-International* **58**, 24–29.

SCHOETENSACK O (1908) Der Unterkiefer des *Homo heidelbergensis* aus den Sanden von Mauer bei Heidelberg. Leipzig: Engelmann.

SCHWARTZ GT, CONROY GC (1996) Cross-sectional geometric properties of the *Otavipithecus* mandible. *American Journal of Physical Anthropology* **99**, 613–623.

SCHWARTZ GT, THACKERAY JF, REID C, VAN REENAN JF (1998) Enamel thickness and the topography of the enamel-dentine junction in South African Plio-Pleistocene hominids with special reference to the Carabelli trait. *Journal of Human Evolution* **35**, 523–542.

SEIDLER H, FALK D, STRINGER C, WILFING H, MUELLER GB, ZUR NEDDEN D et al. (1997) A comparative study of stereolithografically modelled skulls of Petralona and Broken Hill: implications for future studies of middle Pleistocene hominid evolution. *Journal of Human Evolution* **33**, 691–703.

SEMENDEFERI K, DAMASIO H, FRANK R, VAN HOESEN GW (1997) The evolution of the frontal lobes: a volumetric analysis based on three-dimensional reconstructions of magnetic resonance scans of human and ape brains. *Journal of Human Evolution* **32**, 375–388.

SEMENDEFERI K, DAMASIO H (2000) The brain and its main anatomical divisions in living hominoids using magnetic resonance imaging. *Journal of Human Evolution*, in press.

SENUT B (1985) Computerized tomography of a neanderthal humerus from Le Regourdou (Dordogne, France): comparisons with modern man. *Journal of Human Evolution* **14**, 717–723.

SHIBATA T, NAGANO T (1996) Applying very high resolution microfocus x-ray CT and 3-D reconstruction to the human auditory apparatus. *Nature Medicine* **2**, 933–935.

SKINNER MF, SPERBER GH (1982) *Atlas of Radiography of Early Man*. New York: Alan Liss.

SMITH BR (1999) Visualizing human embryos. *Scientific American* March, 58–63.

SMITH BR, JOHNSON GA, GROMAN EV, LINNEY E (1994) Magnetic resonance microscopy of mouse embryos. *Proceedings of the National Academy of Sciences of the USA* **91**, 3530–3533.

SPOOR CF (1993) *The comparative morphology and phylogeny of the human bony labyrinth*. PhD thesis, Utrecht University, The Netherlands.

SPOOR F (1997) Basicranial architecture and relative brain size of Sts 5 (*Australopithecus africanus*) and other Plio-Pleistocene hominids. *South African Journal of Science* **93**, 182–187.

SPOOR CF, ZONNEVELD FW, MACHO GA (1993) Linear measurements of cortical bone and dental enamel by computed tomography: applications and problems. *American Journal of Physical Anthropology* **91**, 469–484.

SPOOR F, WOOD B, ZONNEVELD F (1994) Implications of early hominid labyrinthine morphology for the evolution of human bipedal locomotion. *Nature* **369**, 645–648.

SPOOR CF, ZONNEVELD FW (1994) The bony labyrinth in *Homo erectus*, a preliminary report. *Courier Forschungsinstitut Senckenberg* **171**, 251–256.

SPOOR CF, ZONNEVELD FW (1995) Morphometry of the

primate bony labyrinth: a new method based on high-resolution computed tomography. *Journal of Anatomy* **186**, 271–286.
SPOOR F, LEAKEY M. (1996) Absence of the subarcuate fossa in cercopithecids. *Journal of Human Evolution* **31**, 569–575.
SPOOR F, STRINGER C, ZONNEVELD F (1998) Rare temporal bone pathology of the Singa calvaria from Sudan. *American Journal of Physical Anthropology* **107**, 41–50.
SPOOR F, ZONNEVELD F (1998) A comparative review of the human bony labyrinth. *Yearbook of Physical Anthropology* **41**, 211–251.
SPOOR F, WALKER A, LYNCH J, LIEPINS P, ZONNEVELD F (1998) Primate locomotion and vestibular morphology, with special reference to *Adapis*, *Necrolemur* and *Megaladapis*. *American Journal of Physical Anthropology Supplement* **26**, 207.
SPOOR F, O'HIGGINS P, DEAN C, LIEBERMAN DE (1999) Anterior sphenoid in modern humans. *Nature* **397**, 572.
SPOOR F, ZONNEVELD F (1999) CT-based 3-D imaging of hominid fossils, with notes on internal features of the Broken Hill 1 and SK 47 crania. In *The Paranasal Sinuses of Higher Primates*: *Development*, *Function and Evolution* (ed. Koppe T, Nagai H, Alt KW), pp. 207–226. Berlin: Quintessenz.
SPOOR F, JEFFERY N, ZONNEVELD F (2000) Imaging skeletal growth and evolution. In *Development*, *Growth and Evolution*: *Implications for the Study of the Hominid Skeleton* (ed. O'Higgins P, Cohn M). London: Academic Press, in press.
STEENBEEK JCM VAN KUIJK C GRASHUIS JL (1992) Influence of calibration materials in single- and dual-energy quantitative CT. *Radiology* **183**, 849–855.
STRAIT DS, GRINE FE, MONIZ MA (1997) A reappraisal of early hominid phylogeny. *Journal of Human Evolution* **32**, 17–82.
SWINDELL W, WEBB S (1992) X-ray transmission computed tomography. In *The Physics of Medical Imaging* (ed. Webb S), pp. 98–127. London: IOP.
SWINDLER DR, SIRIANNI JE, TARRANT LH (1973) A longitudinal study of cephalofacial growth in Papio cynocephalus and Macaca nemestrina from three months to three years. *Symposia of the IVth International Congress of Primatology* **3**, 227–240. Basel: Karger
TATE JR, CANN CE (1982) High-resolution computed tomography for the comparative study of fossil and extant bone. *American Journal of Physical Anthropology* **58**, 67–73.
TER HAAR ROMENY BM, ZUIDERVELD KJ, VAN WAES PFGM, VAN WALSUM T, VAN DER WEIJDEN R, WEICKERT J et al. (1998) Advances in three-dimensional diagnostic radiology. *Journal of Anatomy* **193**, 363–371.
THOMPSON JL, ILLERHAUS B (1998) A new reconstruction of the Le Moustier 1 skull and investigation of internal structures using CT data. *Journal of Human Evolution* **35**, 647–665.
TOGA A (1990) *Three-dimensional Neuroimaging*. New York: Raven.
TRINKAUS E, RUFF CB (1989) Diaphyseal cross-sectional morphology and biomechanics of the Fond-de-Forêt 1 femur and the Spy 2 femur and tibia. *Bulletin de la Societé Royale Belge d'Anthropologie Préhistorique* **100**, 33–42.
UDUPA JK, HERMAN GT (1998) *3D Imaging in Medicine*, 2nd edn. Boca Raton: CRC Press.
UDUPA JK, HUNG HM, CHUANG KS (1991) Surface and volume rendering in three-dimensional imaging: a comparison. *Journal of Digital Imaging* **4**, 159–168.
VANNIER MW, CONROY GC, MARSH JL, KNAPP RH (1985) Three-dimensional cranial surface reconstructions using high-resolution computed tomography. *American Journal of Physical Anthropology* **67**, 299–311.
VANNIER MW, CONROY GC (1989) Imaging workstations for computer-aided primatology: promises and pitfalls. *Folia Primatologica* **53**, 7–21.
VANNIER MW, BRUNSDEN BS, HILDEBOLT CF, FALK D, CHEVERUD JM, FIGIEL GS et al. (1991) Brain surface cortical sulcal lengths – quantification with 3- dimensional MR imaging. *Radiology* **180**, 479–484.
WALKER A, LEAKEY R (1988) The evolution of *Australopithecus boisei*. In *Evolutionary History of the 'Robust' Australopithecines* (ed. Grine FE), pp. 247–258. New York: A. de Gruyter.
WARD SC, JOHANSON DC, COPPENS Y (1982) Subocclusional morphology and alveolar process relationships of hominid gnathic elements from Hadar formation: 1974–1977 collections. *American Journal of Physical Anthropology* **57**, 605–630.
WESTBROOK C, KAUT C (1993) *MRI in Practice*. Oxford: Blackwell Scientific.
WILTING JE, ZONNEVELD FW (1997) Computed tomographic angiography. In *Diagnostics of Vascular Diseases* (ed. Lanzer P, Lipton M), pp. 135–153. Berlin: Springer.
WILTING JE, TIMMER J (1999) Artefacts in spiral-CT images and their relation to pitch and subject morphology. *European Radiology* **9**, 316–322.
WIND J (1984) Computerized x-ray tomography of fossil hominid skulls. *American Journal of Physical Anthropology* **63**, 265–282.
WIND J, ZONNEVELD FW (1985) Radiology of fossil hominid skulls. In *Hominid Evolution*, *Past*, *Present and Future* (ed. Tobias PV), pp. 437–442. New York: Alan Liss.
WOOD BA, ABBOTT SA, UYTTERSCHAUT H (1988) Analysis of the dental morphology of Plio-Pleistocene hominids. IV. Mandibular postcanine root morphology. *Journal of Anatomy* **156**, 107–139.
YOUNG SW (1988) *Magnetic Resonance Imaging—Basic Principles*. New York: Raven
ZOLLIKOFER CPE, PONCE DE, LEON MS (1995) Tools for rapid processing in the biosciences *IEEE Computer Graphics and Applications* **16.6**, 148–155.
ZOLLIKOFER CPE, PONCE DE, LEON MS, MARTIN RD, STUCKI P (1995) Neanderthal computer skulls. *Nature* **375**, 283–285.
ZOLLIKOFER CPE, PONCE DE, LEON MS, MARTIN RD (1998) Computer-assisted paleoanthropology. *Evolutionary Anthropology* **6**, 41–54.
ZONNEVELD FW (1987) *Computed Tomography of the Temporal Bone and Orbit*. Munich: Urban and Schwarzenberg.
ZONNEVELD FW (1994) A decade of clinical three-dimensional imaging: a review. Part III. Image analysis and interaction, display options and physical models. *Investigative Radiology* **29**, 716–725.
ZONNEVELD FW, WIND J (1985) High-resolution computed tomography of fossil hominid skulls: a new method and some results. In *Hominid Evolution*, *Past*, *Present and Future* (ed. Tobias PV), pp. 427–436. New York: Alan Liss.
ZONNEVELD FW, SPOOR CF, WIND J (1989) The use of computed tomography in the study of the internal morphology of hominid fossils. *Medicamundi* **34**, 117–128.
ZONNEVELD FW, FUKUTA K (1994) A decade of clinical three-dimensional imaging: a review. Part II. Clinical applications. *Investigative Radiology* **29**, 489–496.
ZUIDERVELD KJ, KONING AHJ, STOKKING R, MAINTZ JBA, APPELMAN FJR, VIERGEVER MA (1996) Multimodality visualization of medical volume data. *Computer Graphics* **20**, 775–791.